

Research Article

Performance Limits of 433 MHz Quarter-wave Monopole Antennas due to Grounding Dimension and Conductivity

Jinfeng Li

Department of Electrical and Electronic Engineering, Imperial College London, United Kingdom

jinfeng.li@imperial.ac.uk

Nuclear Futures Institute, Bangor University, United Kingdom

j.li@bangor.ac.uk

Received: 18th May 2022; Accepted: 14th June 2022; Published: 1st July 2022

Abstract: Among antennas for Industrial, Scientific and Medical (ISM band) applications at 433 MHz, quarter-wave monopole is a reasonably good trade-off between size, gain, and cost. The electrical performance of the monopole is largely dependent on the quality of the ground plane (size and conductivity), which exhibits a practical limit on the achievable gain as most industrial user environments can provide only a finite ground plane of finite electrical conductivity. Establishing traceability in understanding the performance degradation due to such limits due to the grounding dimension and conductivity is becoming mandatory. To this end, this work leverages universal MATLAB in place of off-the-shelf software (HFSS or CST) for the quarter-wave monopole antenna simulation at 433 MHz parametrised with the ground plane's dimension with respect to the wavelength (λ). Results indicate that by enlarging the ground plane's size from 0.14λ to 14λ , the gain (directivity for PEC) from the 3D radiation pattern rises from 1.79 dBi, then starts levelling off at 6.7 dBi (5.78λ), until saturating at 7.49 dBi (13λ). The radiation efficiency and gain of various grounding conductivity scenarios (e.g., gold, aluminium, steel) are also quantified to inform antenna designers and engineers for commercial, industrial, defence and space applications.

Keywords: antenna gain; antenna grounding; antenna modelling; antenna simulation; antenna optimisation; ISM band; MATLAB; monopole antenna; 433 MHz

1. Introduction

Antennas have long been deployed as key components underpinning wireless communications, ranging historically from radar and detection applications oriented for military use cases [1], to nowadays 4G and 5G communications [2], and towards future satellite internet [3] rollout and 6G [4,5]. For more than a century, research into antennas has continuously been captivating researchers from electrical and electronic engineering, as well as materials science [5]. Across the spectrum, compact microstrip antennas at 2.4 GHz have extensively been designed and reported [6], as the frequency dominates the wireless applications in human life (e.g., Wi-Fi, Bluetooth, audio-visual devices, radio control, car alarm, and microwave oven).

Comparatively, 433 MHz of the Industrial, Scientific, and Medical (ISM) band has received very limited attention in terms of device configurations and optimisation possibilities. The wavelength (~ 70 cm) indeed results in huge challenges for antenna miniaturisation (to be as compact as 2.4 GHz devices) whilst upholding a decent gain. Monopole or Yagi antennas are the mainstream solutions at the frequency of 433 MHz, though planar solution (e.g., microstrip patch) is possible at the cost of a big panel size (e.g., ~ 30 cm by 30 cm). Note that miniaturised antennas (e.g., F-inverted [7], fractal [8], photonic bandgap [9], and various bending methods [10,11]) have enabled compact devices at different down-scaling levels, however,

the achievable gain is unacceptably insufficient (normally going negative, e.g., -15 dBi at 433 MHz as reported in [11]) and hence struggling to meet the working range requirements for most wireless remote applications. The push to develop smart sensor networks (e.g., surface acoustic wave sensors array) at 433 MHz (instead of the congested 2.4 GHz), coupled with the absence of experimental proof of reasonably compact antennas with decent gains at this frequency, means that engineering the basic antenna structure is of ongoing research and development interest.

Fundamentally and electromagnetically speaking, the first two key elements of an antenna are the antenna length and impedance matching. While the importance of an antenna's wire (or patch) size and impedance balance is well recognised, there is little work to base the 433 MHz monopole antenna's performance improvement on the grounding plane.

For a quarter-wave monopole antenna (geometry shown in Figure 1 below), a perfect ground plane indicates a perfectly conducting ground with an infinitely large radius, i.e., no leakage and no edge effects. However, such assumptions are unrealistic as the ground plane should always be limited in both area and conductivity. Nevertheless, it is expected that with a bigger ground size, more energy is diverted to a specific direction, i.e., higher directivity.

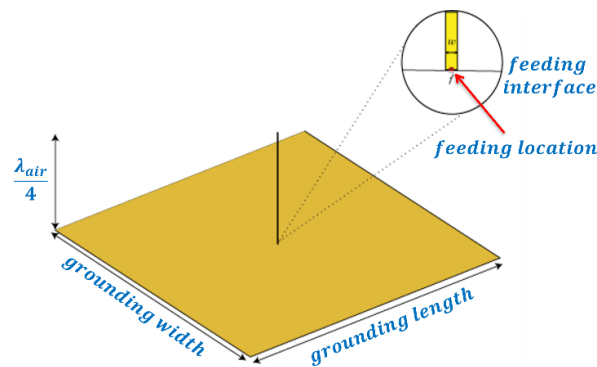


Figure 1. Schematic plot of a quarter-wave monopole antenna model with a zoomed-in monopole rod interface illustrating the feeding position at the geometry centre

On the contrary, the general effect of electrically small ground planes, as well as imperfectly conducting earth grounds, is to tilt the direction of maximum radiation up to higher elevation angles. However, there appears to be limited traceable data to validate and quantify the practice. Nevertheless, for an extreme case that the ground plane is completely not available (i.e., antenna on the earth with highly resistive dry soil), using counterpoise such as radial wires [12] bent downwards demonstrates to partially simulate the ground plane equivalent to a half-wave dipole, though such configuration is out of the scope of this study that assumes a solid ground plane in place.

The structure of the paper encompasses the following sections. Section 2 introduces the modelling methods and assumptions. Section 3 reports the results and analysis, including sub-chapter 3.1 concerning the effect of the grounding plane's dimension on directivity, as well as sub-chapter 3.2 regarding the effect of the grounding plane's conductivity on directivity and gain. Section 4 summarises the novelty and limitations that inspire future investigation.

2. Modelling Methods and Assumptions

Among off-the-shelf software candidates for antenna (and array) simulations, HFSS and CST are arguably the most eminent tools. A range of solvers in HFSS are available, differing in the computation methods, (e.g., FEM, IE, SBR+ Solver, FEBI, IE-Region, DDM, FA-DDM, Transient, CMA, and Eigenmode solvers), while CST is eminent in its time (or frequency) domain solvers based on finite integration techniques (FIT). Compared with HFSS [13] and CST [14] based simulations conducted in our previous works, the MATLAB Antenna toolbox employed in this paper is based on the frequency-domain Method of Moment (MoM) approach, which exhibits a series of advantages, i.e., suitability for quick prototyping, quasi-open source (in low cost), flexibility (in coding and tuning parameters), fast (in particular for array simulations), availability to run programmes online (via the cloud), and ease of communication among

engineers with diverse technical backgrounds. It is well worth noting that existing papers using MoM-based MATLAB codes for antennas development are largely concerning microstrip patch antennas [15,16] at 2.4 GHz, whereas quarter-wave monopole antennas have seldom been reported. In particular, there is a lack of study into 433 MHz monopole using MATLAB, hence the topic is highly motivated to be researched specifically with MATLAB in this work.

Mathematical modelling equations governing this field are well known in the literature [17-19], based on which the most common quarter-wave monopole at 433 MHz is investigated in this work by scripting in MATLAB to model and simulate the grounding dimensional effect on the key performance of the antenna's gain. A symmetric square-shaped metal ground plane is employed and meshed into two-dimensional (2D) triangles, as depicted in the following Figure 2. The zoomed-in region represents the central cylindrical rod of the monopole with a height (length) of a quarter wavelength as per the classic image theory. The continuous surfaces of the metal grounding plane and the antenna rod (vertically placed) are discretized into various adaptive sizes of triangular meshes with the surface current calculations approximated by Rao-Wilton-Glisson [20] basis functions. Note that the non-uniform meshes distribution captures the need for accurately characterize the surface current field of higher gradients, i.e., larger number (and hence finer sizes) of triangular meshes are dedicated to edges, corners and feeding interfaces of the monopole. In the case for dielectrics meshing (out of the scope for this study), three-dimensional (3D) tetrahedrons will be attempted for volumetric meshing. In the current work, however, no dielectrics present for the monopole, hence the metals discretization by surface meshing suffices.

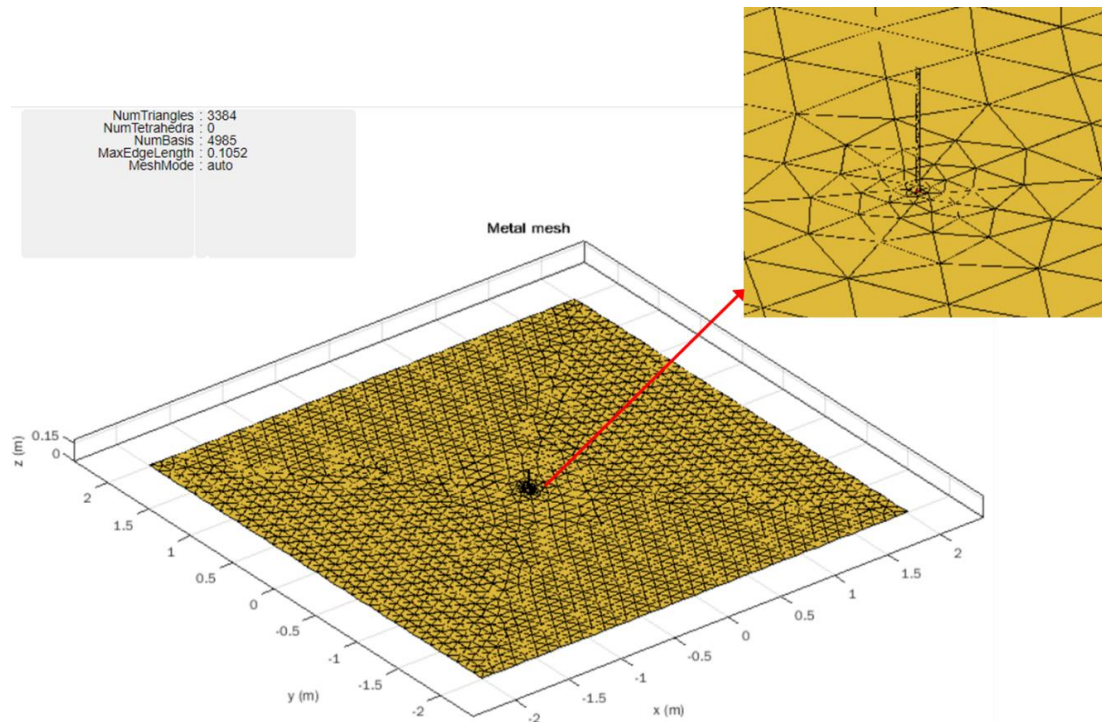


Figure 2. Meshing visualisation for the entire ground plane (top-view) of the quarter-wave monopole antenna model with a zoomed-in monopole rod region (see top right)

To formulate a more detailed understanding of the physics underpinning the grounding dimensional size (area) effect, parameterization of the grounding dimension (area) is firstly performed on a square-shaped grounding plane by only varying the size of the width (and hence the length at the same time), based on which more complex grounding configurations can be targeted and investigated in the future work. To gain fundamental knowledge of the grounding's size effect, the antenna under test is intended to be free from using any special medium (such as tunable dielectrics [21]) or structure (such as metamaterials or photonic bandgaps). Note that conductivity of the ground plane is another independent topic to research, for which we will report in section 3.2. In section 3.1 on studying the ground plane's area effect, we firstly assume a perfect electric conductor (PEC) by default in MATLAB for the ground plane, in which case material losses due to the ground plane can be ignored, i.e., no metal loss and no dielectric losses. With the assumed radiation efficiency of 100%, the antenna's gain problem can thus be reasonably converted to the

directivity investigation interchangeably (regardless of the reflection loss due to impedance mismatch and polarization mismatch loss, though critical in the link calculation but out of scope for this specific study). Note that in MATLAB, the directivity is characterized in the far field at 100 wavelengths away from the antenna.

3. Results, Analysis and Discussions

3.1. Effect of Grounding Plane’s Dimension on Directivity

Results of the 3D radiation pattern and 2D directivity pattern are illustrated in Figure 3, for the grounding dimension of 1λ (wavelength), 3λ , and 10λ , respectively. The complete results of directivity versus the grounding plane’s size are recorded and shown subsequently in Figure 4. Subject to installation limitations, Figure 4 indicates the impact of expanding the ground plane’s dimension from 0.14λ to 14λ . The gain (used interchangeably as directivity for PEC) as obtained from the 3D radiation pattern increases from 1.79 dBi and starts levelling off at 6.7 dBi (5.78λ), until it reaches the fully saturated value of 7.49 dBi (13λ).

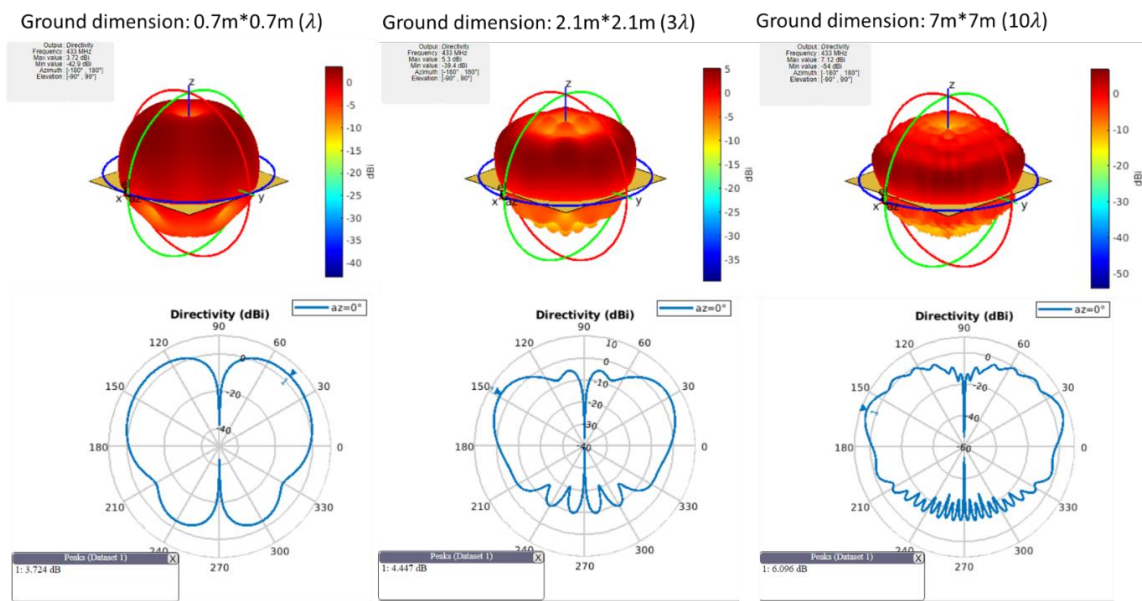


Figure 3. 3D radiation patterns (top row) and 2D pattern ($az=0^\circ$, see bottom row) obtained and analysed at 433 MHz for the quarter-wave monopole (PEC) antenna with exemplary grounding sizes of λ , 3λ and 10λ (from left to right, respectively)

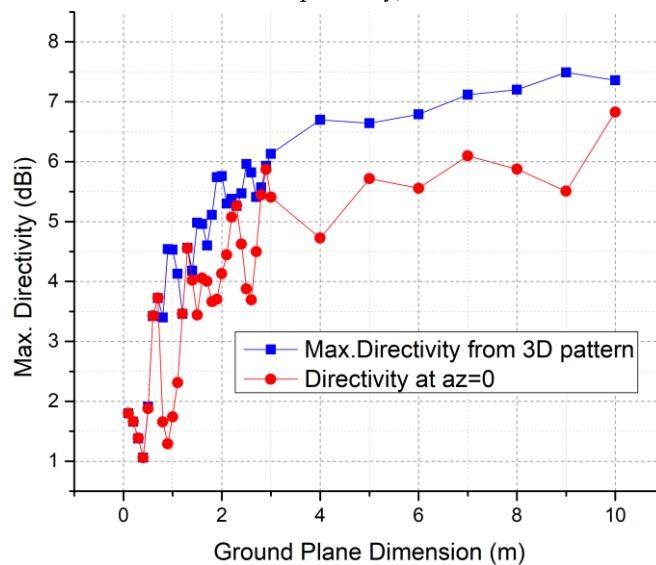


Figure 4. Simulation results of maximum (max.) directivity versus grounding plane size at 433 MHz of the quarter-wave monopole antenna (PEC)

Furthermore, Figure 5 below probes into antenna metrics in terms of lobes visualisation and measurement, including (but not limited to) half-power beamwidth (HPBW), first-null beamwidth (FNBW), front-to-back ratio (F/B), side-lobe level (SLL), maximum main lobe at a specific angle, as well as the maximum back lobe at a corresponding angle (the results of which are detailed within the red box of Figure 5).

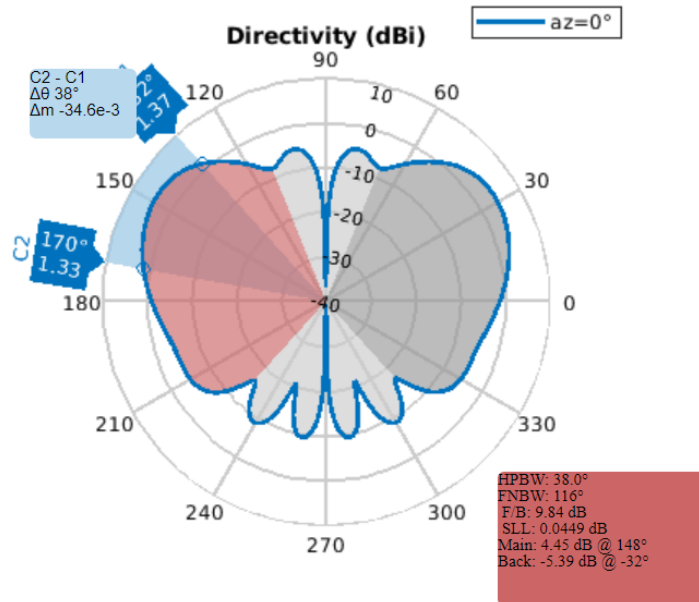


Figure 5. Antenna lobes metrics analysed at 433 MHz for the quarter-wave monopole (PEC) antenna with a ground plane scale of 3λ

Impedance matching is tuned by modifying the feeding position (e.g., the distance away from the centre point), while the resonating frequency is tuned by varying the antenna dimension (length). Figures 6 and 7 report the impedance and reflection loss from 425 MHz to 442 MHz, respectively. The current intensity distribution is plotted in Figure 8. Note that the results of Figures 5-8 are all based on a monopole antenna with a ground plane scale of 3λ by way of illustration. The results visualised in Figure 9 below demonstrate that the near fields of electric (E) and magnetic (H) vector fields can independently exist.

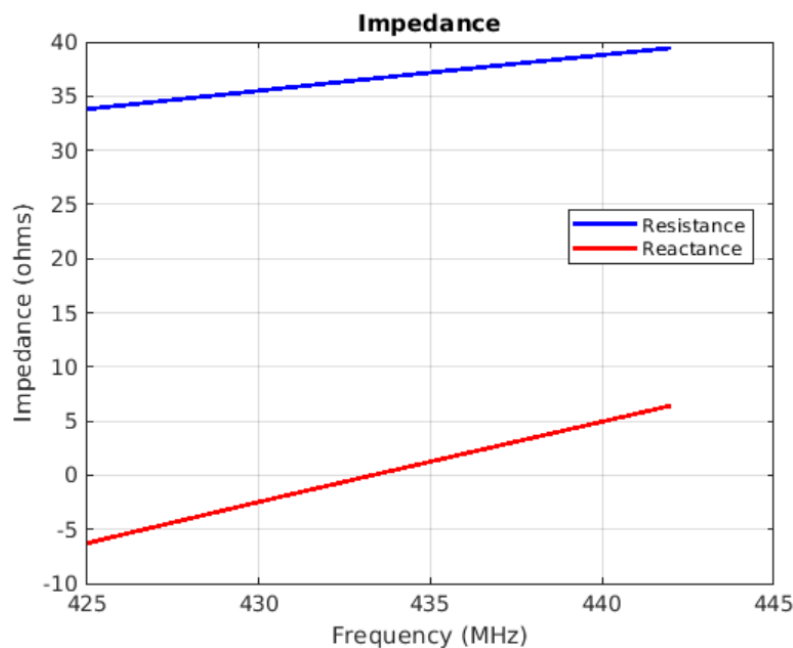


Figure 6. Impedance vs. frequency results illustration of a quarter-wave monopole (PEC) antenna with a ground plane scale of 3λ

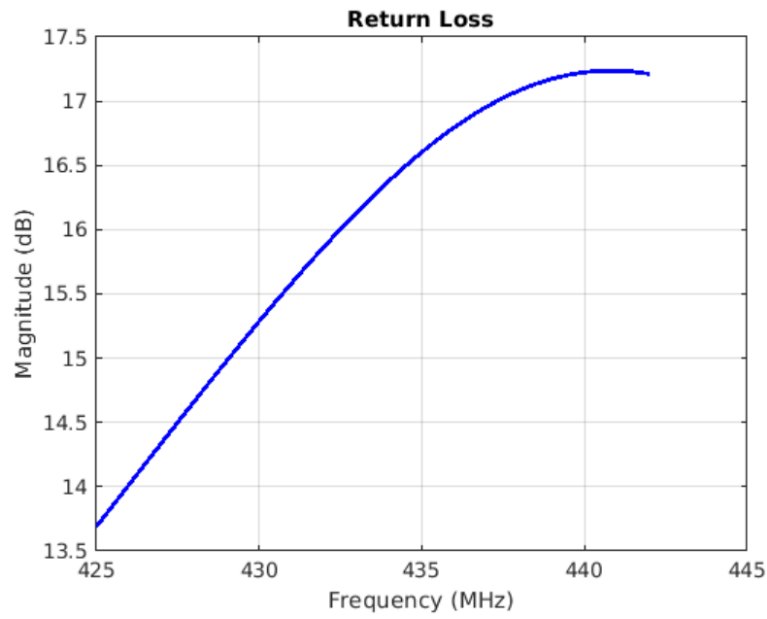


Figure 7. Return loss vs. frequency results illustration of a quarter-wave monopole (PEC) antenna with a ground plane scale of 3λ

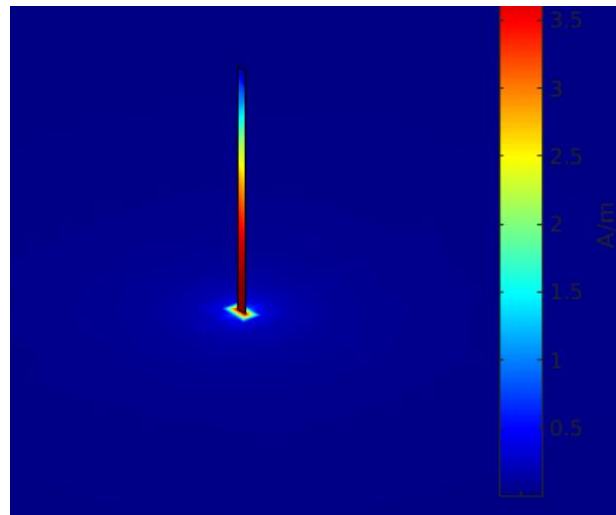


Figure 8. Current distribution plot at 433 MHz of the quarter-wave monopole (PEC) antenna with a ground plane dimension of 3λ

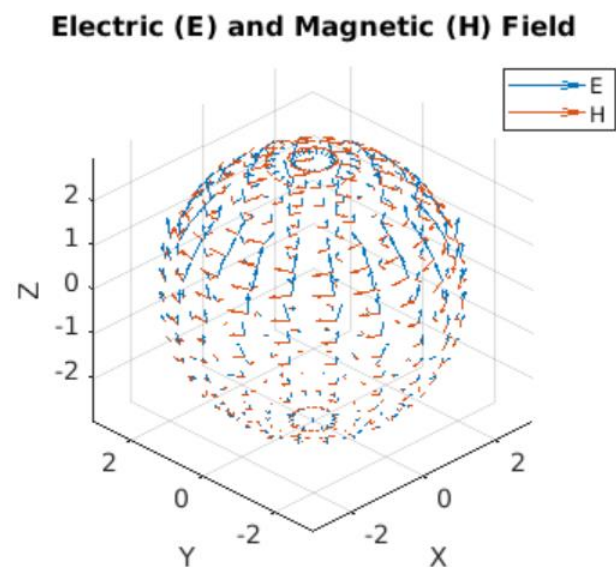


Figure 9. Near-field visualisation of the electric and magnetic fields at 433 MHz for the monopole antenna with a ground plane dimension of 3λ

3.2. Effect of Grounding Plane's Conductivity on Directivity and Gain

Another main contribution of this research is to quantify the impact of the grounding plane's electrical conductivity on the directivity and gain of a single monopole antenna, respectively. The same quarter-wave monopole antenna topology as above is investigated by varying the ground plane's materials (ranging from PEC, silver, copper, gold, aluminium, tungsten, zinc, brass, iron, steel, and lead), whilst maintaining the same geometry and dimension. Here the square grounding plane's dimension is selected as 4 m (i.e., the saturating threshold size as observed from section 3.1) to minimise the unstable effect due to the ground plane's area and also to reduce the computation burden. The script is briefed in Figure 10 below. Similar to section 3.1, both the maximum directivity from the 3D radiation pattern and the directivity at the 2D plane of $az=0$ (azimuth) are analysed and illustrated in Figure 11.

```
%effect of ground plane conductivity on directivity and gain
m = metal('steel')
pc=monopole('Conductor',m,'Height',0.1627,'Width',0.0069,'GroundPlaneLength',4,'GroundPlaneWidth',4,...
'FeedOffset',[0 0],'Tilt', 0,'TiltAxis',[0 1 0])
show (pc)
Z=impedance(pc,433e6)
RL=returnLoss(pc,433e6)
E=efficiency(pc,433e6)
%current(pc,433e6)
figure
pattern(pc,433e6)
figure
pattern(pc,433e6,0,0:1:360) %az=0,elevation from 0 to 360
pattern_max = max(max(pattern(pc,433e6)))
T = table(Z,RL,pattern_max,E)
writetable(T,'steel.txt')
```

Figure 10. Scripting in MATLAB for the quarter-wave monopole antenna's modelling, calculations, and patterns visualisation

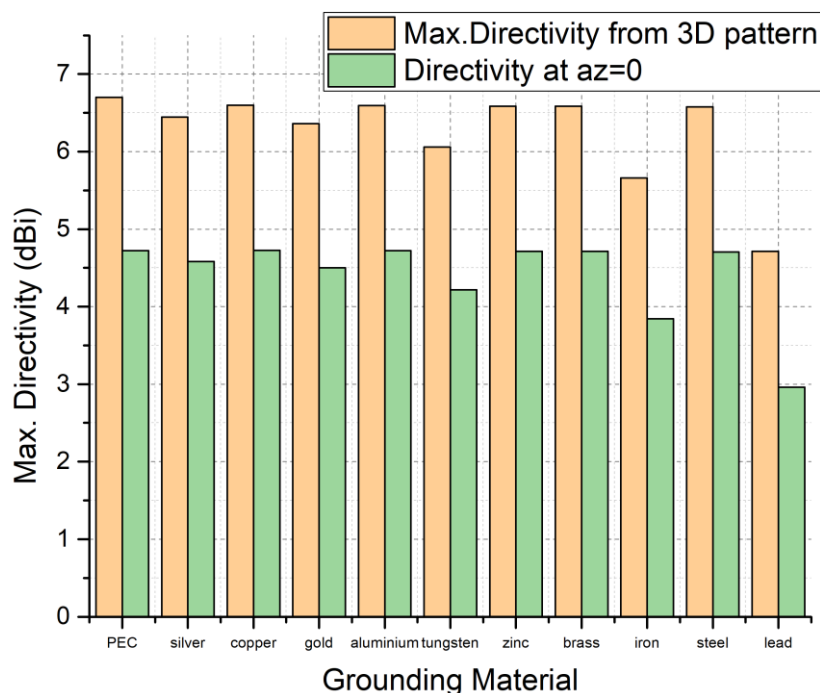


Figure 11. Simulated maximum (max.) directivity at 433 MHz of the quarter-wave monopole antenna with diverse grounding conductors of the same device dimension

As distinct from the concept of an antenna's gain, directivity is independent of dielectric and metal ohmic losses. Accordingly, the directivity results in Figure 11 have nothing to do with the various metal losses due to different finite conductive materials utilised. However, the conductivity of the grounding material does affect the directivity by tilting the maximum radiation pattern and hence the maximum radiation intensity. The newly derived results of gain versus materials of different finite conductivity are presented in Figure 13 by multiplying the directivity (Figure 10) with the obtained antenna efficiency (Figure 12).

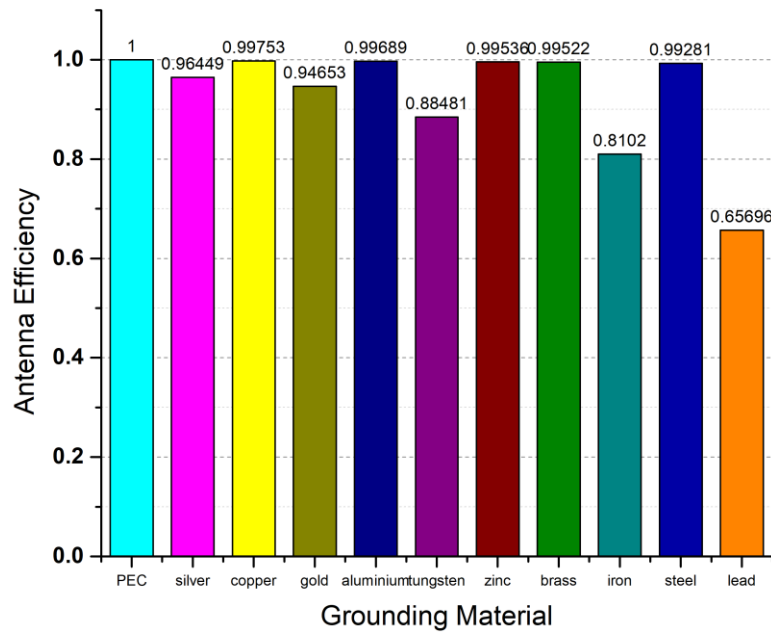


Figure 12. Simulated antenna efficiency at 433 MHz of the quarter-wave monopole antenna with diverse grounding conductors of the same device dimension

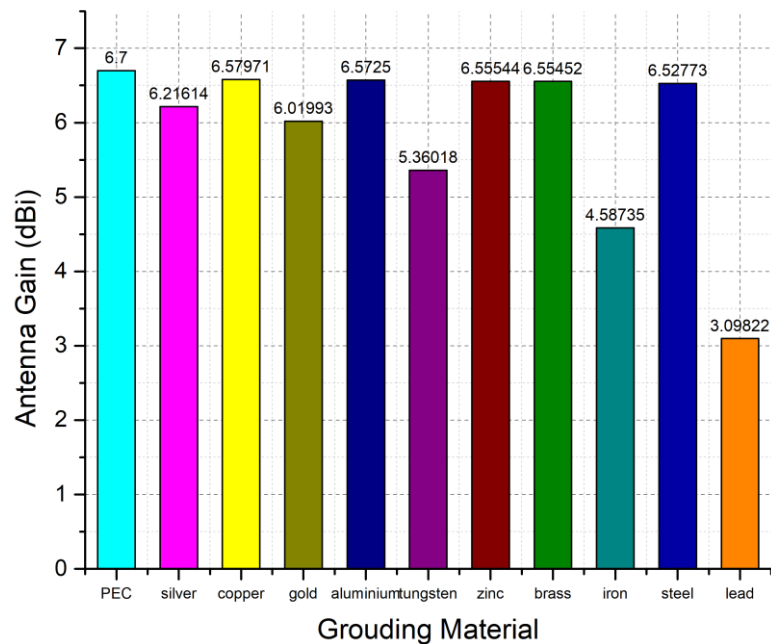


Figure 13. Simulated gain at 433 MHz of the quarter-wave monopole antenna with diverse grounding materials of the same device dimension

Benchmarking the results of the ideal PEC grounding (infinite conductivity with a radiation efficiency of 100%), the degradations of antenna gain due to using copper, aluminium, zinc, brass, or steel grounding are all less than -0.2 dBi at 433 MHz. However, the degradations are higher for those based on silver (-0.5 dBi), gold (-0.7 dBi), tungsten (-1.3 dBi), and becoming significant for those grounded with iron (-2.1 dBi) and lead (-3.6 dBi) at 433 MHz. The implications of such quantified performance degradation due to the grounding materials can inform decision-making in a wide range of commercial applications such as the optimisation of materials for vehicular antennas [22-24].

In addition to the conventional vehicular antenna application that can be foreseen, the insights are also transferrable towards emerging industry applications at 433 MHz such as wireless passive monitoring of instrumentation and process control for chemistry and nuclear power plants. This work also demonstrates the added value of cost-effective synergy leveraging the availability of a universal software platform (i.e., MATLAB) for antenna hardware research and development.

Limitations do exist as the quarter-wave monopole studied in this work is squarely symmetric by geometry (essentially a one-dimensional parametric representation instead of two-dimensional). Future

work could investigate possibilities of cylindrically symmetric by geometry, as well as more non-uniformly shaped grounding (e.g., triangular, rectangular, elliptical), the results of which will inform follow-up iterations of experiments (fabrication, assembly, and measurement) for the antenna's performance optimisation.

4. Conclusion

This work quantifies the effects of the grounding plane on the directivity (and gain) of quarter-wave monopole antennas at 433 MHz. Method of Moments-based MATLAB programmes are developed, the simulations from which are replacing those from off-the-shelf software such as Ansys HFSS and CST. Various facets of grounding characteristics are investigated, including the grounding plane's area and conductivity. The results are of both fundamental and practical importance for antenna device design and materials selection at 433 MHz. Furthermore, the new quantitative data obtained in this work is insightful for understanding the performance limits of monopole antennas in service or prior to calibration, inspired by which a more proper calibration or compensation action can be taken for continuing performance gains towards the maximally achievable operation.

Acknowledgement

The author would like to acknowledge Bangor University for housing the MATLAB Online versatile development environment for conducting the simulation. No potential conflict of interest was reported by the author.

References

- [1] Rob Lewis, "Wideband antenna technology in military applications", in *International Workshop on Antenna Technology (iWAT)*, 2010, Lisbon, pp. 1-4. DOI: 10.1109/IWAT.2010.5464655.
- [2] Khalil H. Sayidmarie, Neil J. McEwan, Peter S. Excell, Raed A. Abd-Alhameed and Chan H. See, "Antennas for emerging 5G systems", *International Journal of Antennas and Propagation*, Vol. 2019, 9290210, 2019. DOI: 10.1155/2019/9290210.
- [3] Jinfeng Li, "All-optically controlled microwave analog phase shifter with insertion losses balancing", *Engineering Letters*, Published by International Association of Engineers (IAENG), Vol. 28, No. 3, pp. 663-667, September 2020. Available: http://www.engineeringletters.com/issues_v28/issue_3/EL_28_3_03.pdf.
- [4] Zahraa R.M. Hajiyat, Alyani Ismail, Aduwati Salia and Mohd. Nizar Hamidon, "Antenna in 6G wireless communication system: Specifications, challenges, and research directions", *Optik (Stuttg)*, Vol. 231, 166415, April 2021, DOI: 10.1016/j.ijleo.2021.166415.
- [5] Jinfeng Li, "Optically steerable phased array enabling technology based on mesogenic azobenzene liquid crystals for starlink towards 6G", in *2020 IEEE Asia-Pacific Microwave Conference (APMC)*, 2020, Hong Kong, pp. 345-347, DOI: 10.1109/APMC47863.2020.9331345.
- [6] V. Asokan, S. Thilagam and K. Vinoth Kumar, "Design and analysis of microstrip patch antenna for 2.4GHz ISM band and WLAN application", in *2015 2nd International Conference on Electronics and Communication Systems (ICECS)*, 2015, Coimbatore, India, pp. 1114-1118. DOI: 10.1109/ECS.2015.7124756.
- [7] Cheuk Yin Cheung, Joseph S.M. Yuen and Steve W.Y. Mung, "Miniaturized printed inverted-F antenna for Internet of things: A design on PCB with a meandering line and shorting strip", *International Journal of Antennas and Propagation*, Vol. 2018, 5172960, pp. 1-5, March 2018, DOI: 10.1155/2018/5172960.
- [8] Dmitrii Tumakov, Dmitry Chikrin and Petr Kokunin, "Miniaturization of a Koch-type fractal antenna for WI-Fi applications", *Fractal and Fractional*, Vol. 4, 25, June 2020, DOI: 10.3390/fractalfract4020025.
- [9] Mohamed Nasr Eddine Temmar, Abdesselam Hocini, Djamel Khedrouche and Mehdi Zamani, "Analysis and design of a terahertz microstrip antenna based on a synthesized photonic bandgap substrate using BPSO", *Journal of Computational Electronics*, Vol. 18, pp. 231-240, January 2019, DOI: 10.1007/s10825-019-01301-x.
- [10] Jinfeng Li, "Bias tees integrated liquid crystals inverted microstrip phase shifter for phased array feeds", in *2020 21st International Conference on Electronic Packaging Technology (ICEPT)*, pp. 1-5, September 2020, DOI: 10.1109/ICEPT50128.2020.9202604.
- [11] A. Babar, L. Ukkonen, M. Soini and L. Sydanheimo, "Miniaturized 433 MHz antenna for card size wireless systems", in *2009 IEEE Antennas and Propagation Society International Symposium*, pp. 1-4, July 2009, DOI: 10.1109/APS.2009.5171803.

- [12] Mahdi Fartookzadeh, Seyyed Hossein, Mohseni Armaki, Seyyed Mohamad Javad Razavi and Jalil Rashed-Mohasse, "Optimum Functions for Radial Wires of Monopole Antennas with Arbitrary Elevation Angles", *Radioengineering*, Vol. 25, No. 1, April 2016, DOI: 10.13164/re.2016.0053.
- [13] Jinfeng Li, "Towards 76-81 GHz Scalable Phase Shifting by Folded Dual-strip Shielded Coplanar Waveguide with Liquid Crystals", *Annals of Emerging Technologies in Computing (AETiC)*, Print ISSN: 2516-0281, Online ISSN: 2516-029X, pp. 14-22, Vol. 5, No. 4, 1st October 2021, Published by International Association of Educators and Researchers (IAER), DOI: 10.33166/AETiC.2021.04.002, Available: <http://aetic.theiaer.org/archive/v5/v5n4/p2.html>.
- [14] Jinfeng Li, "Wideband PCB-to-connectors impedance adapters for liquid crystal-based low-loss phase shifters", in *2020 50th European Microwave Conference (EuMC)*, Utrecht, Netherlands, pp. 546-549, February 2021, DOI: 10.23919/EuMC48046.2021.9337967.
- [15] Aniket Puranik, Swapnajeet Nayak, Atul Agnihotri, Abhay Visoriya, Shubham Chouhan, S.K. Jain and Chandresh Dhote, "Design of microstrip patch antennas using method of moment based MATLAB codes", in *2017 International Conference on Information, Communication, Instrumentation and Control (ICICIC)*, Indore, India, pp. 1-4, February 2018, DOI: 10.1109/ICOMICON.2017.8279068.
- [16] S.N.S. Mahmud, M.A. Jusoh, S.E. Jasim, A.H. Zamani and M.H. Abdullah "Design, simulation and analysis a microstrip antenna using PU-EFB substrate", *IOP Conference Series: Materials Science and Engineering*, Vol. 342, 012021, 2018, DOI: 10.1088/1757-899X/342/1/012021.
- [17] A. Rashid, "Quasi-near-zone field of a monopole antenna and the current distribution of an antenna on a finite conductive earth", in *IEEE Transactions on Antennas and Propagation*, Vol. 18, No. 1, pp. 22-28, January 1970, DOI: 10.1109/TAP.1970.1139616.
- [18] B. Turetken, "Monopole antenna calibration in GTEM cell", in *10th International Conference on Mathematical Methods in Electromagnetic Theory*, pp. 298-300, September 2004, DOI: 10.1109/MMET.2004.1397016.
- [19] A.W.C. Chu, S. A. Long and D. R. Wilton, "The radiation pattern of a monopole antenna attached to a conducting box", *IEEE Transactions on Antennas and Propagation*, Vol. 38, No. 12, pp. 1907-1912, December 1990, DOI: 10.1109/8.60978.
- [20] Sadasiva M. Rao, Donald R. Wilton and Allen W. Glisson, "Electromagnetic scattering by surfaces of arbitrary shape", *IEEE Transactions on Antennas and Propagation*, Vol. 30, No. 3, pp. 409-418, May 1982, DOI: 10.1109/TAP.1982.1142818.
- [21] Jinfeng Li, "Challenges and Opportunities for Nematic Liquid Crystals in Radio Frequency and Beyond", *Crystals*, Vol. 12, No. 5, 632, April 2022, DOI: 10.3390/cryst12050632.
- [22] A.R. Ruddle, "Simulation of far-field characteristics and measurement techniques for vehicle-mounted antennas", *IEE Colloquium on Antennas for Automotives*, London, UK, pp. 7/1-7/8, August 2002, DOI: 10.1049/ic:20000007.
- [23] Gerald Artner, Robert Langwieser and Christoph F. Mecklenbräuker, "Material induced changes of antenna performance in vehicular applications", in *2015 IEEE International Conference on Microwaves, Communications, Antennas and Electronic Systems (COMCAS)*, Tel Aviv, Israel, pp. 1-4, December 2015, DOI: 10.1109/COMCAS.2015.7360442.
- [24] S. Bandi, B.T.P. Madhav, D.K. Nayak and S.S.M. Reddy, "Compact flexible inkjet-printing antenna on paper and transparent PET substrate materials for vehicular instrument communication", *Journal of Instrumentation*, Vol. 14, October 2019, DOI: 10.1088/1748-0221/14/10/P10022.



© 2022 by the author(s). Published by Annals of Emerging Technologies in Computing (AETiC), under the terms and conditions of the Creative Commons Attribution (CC BY) license which can be accessed at <http://creativecommons.org/licenses/by/4.0>.